Atherosclerosis 285 (2019) 23–30

Contents lists available at ScienceDirect

Atherosclerosis

journal homepage: www.elsevier.com/locate/atherosclerosis

Akebia Saponin D inhibits the formation of atherosclerosis in *ApoE*$^{-/-}$ mice by attenuating oxidative stress-induced apoptosis in endothelial cells

Song Yang, Wen Zhang, Ling-ling Xuan, Fei-fei Han, Ya-li Lv, Zi-rui Wan, He Liu, Lu-lu Ren, Li-li Gong*, Li-hong Liu**

Beijing Chao-Yang Hospital, Capital Medical University, Beijing, 100020, China

HIGHLIGHTS

- Akebia Saponin D inhibits oxidative stress-induced apoptosis in human umbilical vein endothelial cells.
- Akebia Saponin D ameliorates lipid metabolism and inhibits lipid deposition in the liver and vascular tissue.
- Akebia Saponin D inhibits the formation of atherosclerotic plaque in *ApoE*$^{-/-}$mice.

ARTICLE INFO

Keywords:
Atherosclerosis
Akebia saponin D
Antioxidant
Apoptosis

ABSTRACT

Background and aims: Akebia Saponin D (ASD) is a major bioactive triterpenoid saponin compound isolated from the Chinese herb Dipsacus asper wall (DSW). DSW has been long used as an anti-Alzheimer disease and anti-osteoporosis agent in clinics. However, anti-atherosclerotic effects of ASD have not been fully investigated. The objective of this study is to further investigate the anti-atherosclerotic activities and mechanisms of ASD *in vivo* and *in vitro*.

Methods: In *in vitro* experiments, ASD (50, 100, and 200 μM) was used to explore the effects of preventing H_2O_2-induced endothelial cell apoptosis and the possible mechanism involved. In *in vivo* experiments, *ApoE*$^{-/-}$ mice were fed a high fat diet (HFD) and treated with atorvastatin (10 mg/kg/d), ASD (50, 150, 450 mg/kg/d), or the combination therapy (atorvastatin 10 mg/kg/d and ASD 150 mg/kg/d) for 14 weeks.

Results: We found that ASD reduced the generation of reactive oxygen species, inhibited mitochondrial membrane potential (MMP) impairment, diminished the expression of Bax and Caspase-3, increased Bcl-2 expression, and inhibited apoptosis in endothelial cells. ASD significantly increased the expression of anti-oxidant enzymes (GSH, SOD, and CAT) in both liver and vascular tissue, reduced blood lipid levels (TG, TC, and LDL-C), and decreased lipid deposition in the liver and atherosclerotic lesion size in *ApoE*$^{-/-}$ mice.

Conclusions: Our study revealed that ASD inhibited atherosclerosis development in *ApoE*$^{-/-}$ mice by inhibiting oxidative stress-induced endothelial cell apoptosis signaling pathway, and suggested that ASD might be a potential therapeutic drug in the prevention of atherosclerosis.

1. Introduction

Cardiovascular disease (CVD) has produced immense health and economic burdens globally. Coronary heart disease (CHD) is the leading cause of deaths (43.8%) attributable to CVD [1]. Atherosclerosis (AS) has become the leading cause of CHD in western developed countries characterized by its high morbidity and mortality [2].

Atherosclerosis (AS) is a complex pathological condition among vascular diseases, which is characterized by accumulation of lipids and plaque formation in large arteries [3]. Atherosclerosis has now been regarded as a chronic inflammatory disease of the arterial wall [4,5]. Endothelial dysfunction is a starting step of AS [6]. After that, the circulating monocytes adhere to the intima, move to the injured wall, differentiate into macrophages, and then, swallow modified LDL-C to form early atherosclerosis lesions. Among many risk factors, oxidative stress is considered as a primary event involved in the initiation and progression of endothelial dysfunction [7]. Oxidative stress enhances the production of ROS, which stimulates the expression of cell adhesion

* Corresponding author. Beijing Chaoyang Hospital, Capital Medical University, 8 Gongren Tiyuchang Nanlu, Beijing 100020, China.
** Corresponding author. Beijing Chaoyang Hospital, Capital Medical University, 8 Gongren Tiyuchang Nanlu, Beijing 100020, China.
E-mail addresses: gonglili@126.com (L.-l. Gong), hongllh@126.com, liulihong@bjcyh.com (L.-h. Liu).

https://doi.org/10.1016/j.atherosclerosis.2019.04.202
Received 15 October 2018; Received in revised form 21 February 2019; Accepted 3 April 2019
Available online 10 April 2019
0021-9150/

molecule (CAM) in endothelial surface. CAM produced by endothelial cells plays a role in trapping monocytes/macrophages into the vessel wall, subsequently resulting in foam cell formation and atherosclerosis [8]. Under pathological conditions, most of the intracellular reactive oxygen species (ROS) generate from mitochondrial dysfunction [9,10]. Accumulation of ROS due to unbalanced mitochondrial membrane potential activates caspase-dependent apoptotic signaling pathways, directly leading to cellular apoptosis [11]. As it is already known, H_2O_2 is the most potent ROS stimulant involved in intracellular signaling, which has also been extensively used to study oxidative stress in *in vitro* models [12]. Accordingly, there is growing evidence that suggests that the endothelial dysfunction is a potential target for early prevention and treatment of atherosclerosis, although the current therapeutic strategies are still primarily focusing on lowering LDL-C [13].

In recent years, researchers have found many herbal medicines, which exhibit anti-oxidant effects on ischemic heart diseases. Akebia saponin D (ASD, also named as Asperosaponin VI) (Supplementary Fig. 1) is a triterpenoid saponin extracted from a traditional Chinese medicine, the root of Dipsacus asper Wall. Pharmacological studies have indicated that ASD exhibits several biological activities, such as anti-osteoporosis, anti-acute myocardial infarction, anti-Alzheimer disease (AD), and so on [14–16]. Meanwhile, our group has demonstrated that ASD inhibited the deposition of lipids in the liver and the formation of the nonalcoholic fatty liver in *ob/ob* mice [17]. Thus, we predicted that ASD could inhibit atherosclerosis by ameliorating metabolic disorders. However, the cardiovascular protective effects of ASD have not been thoroughly elucidated.

Therefore, the present study aimed to observe the effects of ASD on H_2O_2-induced endothelial cell apoptosis. The current study also evaluated the therapeutic potential of ASD during atherogenesis in the *ApoE*$^{-/-}$ mice.

2. Materials and methods

2.1. Materials

ASD was purchased from Sigma Aldrich (St. Louis, MO, USA). Fetal bovine serum (FBS) and Dulbecco's Modified Eagle Medium/F12 (DMEM/F12) was obtained from Hyclone (Logan, Utah, USA). H_2O_2 was obtained from Union-Bio Technology (Beijing, China). Cell Counting Kit-8 (CCK-8) was purchased from Salarbio Molecular Technologies (Beijing, China). The kits for determining superoxide dismutase (SOD), reduced glutathione (GSH), catalase (CAT), total cholesterol (TC), triglyceride (TG), low-density lipoprotein cholesterol (LDL-C), alanine aminotransferase (ALT), and aspartate aminotransferase (AST) are purchased from Nanjing Jiancheng Institute of Biological Engineering (Nanjing, China). 3-amino,4-aminomethyl-2′,7′-difluorescein, diacetate (DAF-FM DA) and 2′,7′-dichlorofluorescein diacetate (DCFH-DA), and 5,5′,6,6′-tetrachloro-1,1′,3,3′-tetraethylbenzimidazolcarbocyanine iodide (JC-1) were obtained from Beyotime Biotechnology (Shanghai, China). Annexin V-fluorescein isothiocyanate (FITC)/propidium iodide (PI) apoptosis detection kits were purchased from KeyGen Biotech (Nanjing, China). Antibodies against Bax, Bcl-2, caspase-3, and GAPDH were obtained from Cell Signaling Technology. Immobilon PVDF membrane was purchased from Millipore (Billerica, MA, USA).

2.2. Cell culture and treatment

Human umbilical vein endothelial cells (HUVECs) were purchased from ATCC (American Type Culture Collection, USA). HUVECs were grown in DMEM/F12, supplemented with 10% FBS. Cells were incubated in a humidified incubator with 5% CO_2 at 37 °C with media replenishment after every 2 days and were passaged at 80–90% confluence. To assess the effect of ASD on H_2O_2-induced HUVEC injury, cells are divided into following groups: the vehicle control group, the ASD group (200 μM ASD), the H_2O_2 group (300 μM H_2O_2), and the protection group (50,100, or 200 μM ASD + 300 μM H_2O_2).

2.2.1. Cell viability and apoptosis

2.2.1.1. Cell viability assay. To measure cell viability, HUVECs were analyzed by CCK-8 assay. HUVECs were plated within 96-well plates at a density of 10^4 cells/well and incubated in DMEM/F12 supplemented with 10% FBS, and then, incubated for 12 h at 37 °C. After 12 h, the cells were pretreated with 50, 100, and 200 μM ASD in no serum media for 12 h, following which 300 μM H_2O_2 was added into the media containing ASD and the cells were further cultured for 24 h. The viability of cells treated with ASD (50, 100, and 200 μM) and H_2O_2 alone (200–400 μM) were also assessed. Then, 10 μL CCK-8 reagent was added to each well and wavelength was evaluated at 450 nm in a spectrophotometer. Each experiment was repeated in five wells and was duplicated for at least three times.

2.2.1.2. DAPI staining. The morphological characteristics of the nucleus were observed by DAPI staining. HUVECs were seeded in a 6-well plate at a density of 1×10^5/mL cells. After 12 h, cells were pretreated with indicated concentrations of ASD (50, 100, 200 μM), and then they were stimulated with H_2O_2 (300 μM) for 24 h. After incubation, the cells were stained with DAPI. The stained cells were visualized under an inverted fluorescence microscope (CKX4, OLYMPUS, Japan).

2.2.1.3. Apoptosis analysis by flow cytometry. Flow cytometric analysis was performed to identify and quantify the apoptotic cells using Annexin V- FITC/PI staining detection kit. HUVECs (1×10^5/mL) were cultured in 6-well plates. After the same protective treatment, flow cytometry was performed using a FACS Calibur (BD, USA). Data were analyzed using Cell Quest software (Becton–Dickinson). The degree of apoptosis was determined as the percentage of annexin V-positive cells/PI-negative cells.

2.2.2. Measurement of mitochondrial membrane potential (MMP, $\triangle\Psi m$)

Mitochondria play a key role in cell apoptosis, and the disruption of mitochondrial membrane potential (ΔΨm) is an early signal in apoptotic cascade. In cells, JC-1 accumulates in the mitochondria as aggregates (red) when the MMP is at a high level, whereas it would be cleaved as a monomer (green) if the MMP was disrupted. Briefly, HUVECs (1×10^5/mL) were seeded in 6-well plates overnight. Then, after the same treatment, cells were incubated with 0.5 μM JC-1 for 15 min. Subsequently, samples were assessed using a florescence microscopy.

2.2.3. ROS assay

To analyze the generation of ROS, DCFH-DA staining was used to detect cytoplasmic ROS. HUVECs (1×10^5/mL) were seeded in 12-well plates. After the same protective treatment, cells were stained with DCFH-DA. Fluorescent images were captured by an inverted fluorescence microscope and analyzed by Image-Pro software.

2.3. Mice

Male C57BL/6 and *ApoE*$^{-/-}$ mice (six-week-old and weighing 20 ± 2 g) were purchased from Beijing Vital River Laboratory Animal Technology. *ApoE*$^{-/-}$ mice were fed with high-fat diet during the entire experimental period. The food composition of the high-fat diet included 15% cocoa butter and 0.5% cholesterol. C57BL/6 mice were fed with standard chow. All of the animal experiments followed the instructions of the Laboratory Animal Management Statute of China Physiological Society and were approved by the Beijing Chao-Yang Hospital Committee on Ethics in the Care and Use of Laboratory Animals. All animals were maintained in a temperature and humidity-controlled facility under standard conditions, and provided with water

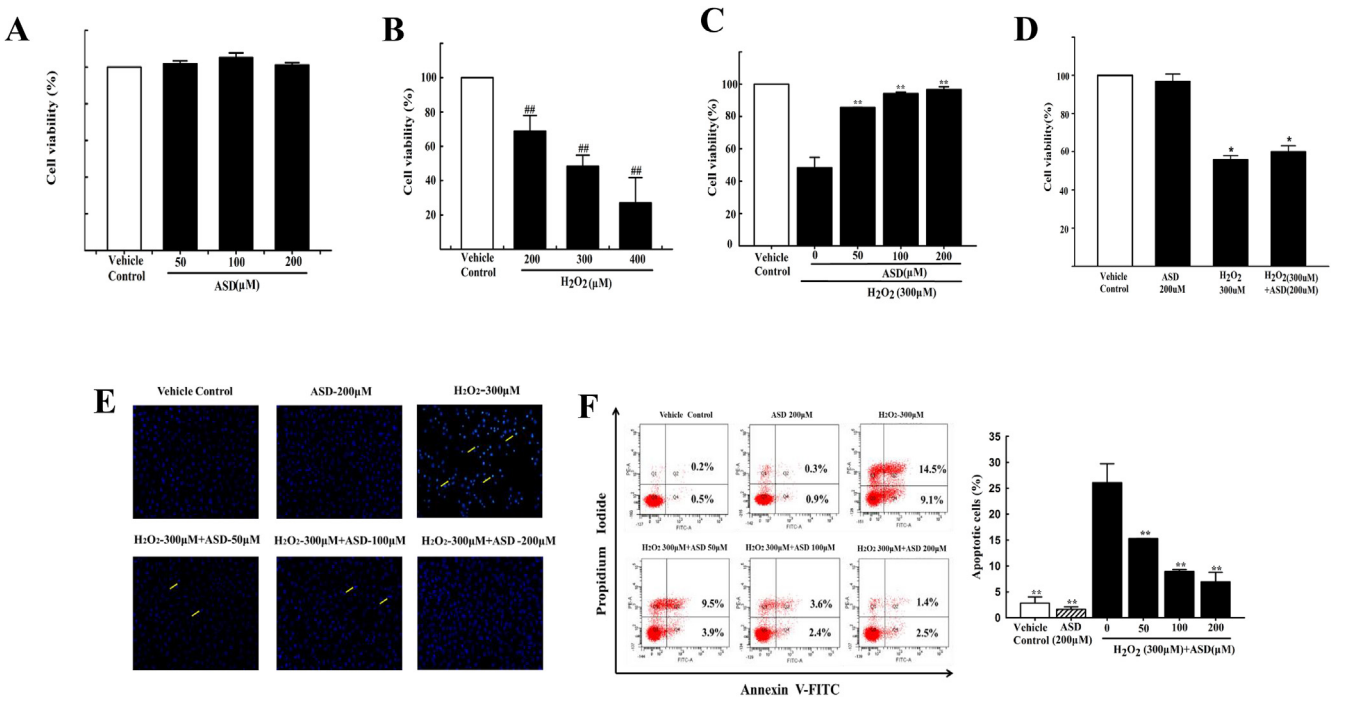

Fig. 1. ASD protects HUVECs against H_2O_2-induced cytotoxicity and apoptosis.
(A) HUVECs were incubated with the indicated concentrations of ASD for 24 h and cell viability was determined. (B) HUVECs were incubated for 24 h with H_2O_2 (200, 300, and 400 μM). Cell viability was analyzed using CCK-8 assay. (C) HUVECs were pretreated with ASD (50, 100, or 200 μM) for 12 h, and then treated with H_2O_2 (300 μM) for 24 h; cell viability was assayed with a CCK-8 assay. (D) HUVECs were treated with H_2O_2 (300 μM), ASD (200 μM), H_2O_2 (300 μM) + ASD (200 μM) simultaneously and cell viability was determined. (E) Nuclear condensation (arrows) was evaluated by DAPI staining. (F) Flow cytometry of H_2O_2-induced apoptosis following Annexin V-FITC/PI double staining. Statistical analysis of the proportions of HUVECs corresponding to early and late apoptotic cells. Data are presented as mean ± SEM. $^{\#\#}p < 0.01$ compared with the control group; $^{**}p < 0.01$ compared with the H_2O_2-treated group (n = 3).

ad libitum. After 1 week of accommodation, $ApoE^{-/-}$ mice were randomly divided into the following six groups (n = 10 in each group): 1) $ApoE^{-/-}$ model group; 2) ASD 50 mg/kg/d; 3) ASD 150 mg/kg/d; 4) ASD 450 mg/kg/d; 5) Atorvastatin 10 mg/kg/d; 6) Combine treatment: ASD 150 mg/k/d + Atorvastatin 10 mg/kg/d.

2.3.1. Biochemical indexes assay

Mice were fasted overnight and blood samples were collected from the retroorbital plexus. Serum was obtained by centrifugation at 3000 rpm for 10 min at 4 °C, and then, kept frozen at −80 °C until further analysis. Serum levels of ALT, AST, TC, TG, and LDL-C were measured by commercial enzymatic methods, according to the manufacturer's instructions. Antioxidant enzymes (GSH, SOD, and CAT) in vascular tissues and liver were measured as described before.

2.3.2. Hematoxylin-eosin (H&E) staining

The isolated liver and vascular tissues were washed with PBS three times and fixed with 4% paraformaldehyde. Paraffin sections were cut at 5 μm-thickness and stained with hematoxylin and eosin (H&E). Microscopic examination was performed with H&E stain to assess fatty changes in liver and atherosclerotic changes in the aorta. Atherosclerotic lesions were measured on digital microphotographs and the percentage of plaque surface area was calculated using ImageJ software. Results were expressed as a percentage of total vascular area covered with atherosclerotic lesions.

2.3.3. Oil Red O staining

To determine the severity of the lesions and quantify the atherosclerotic burden, we measured the surface area of the Oil Red O-positive lesions on the surface of whole aortas. Opened lengthwise and edges and corners were flatted on black boards. For en face analyses of lesions in the entire aorta, the plaque was evaluated based on Oil Red O staining using Image-Pro Plus. Statistics on hepatic steatosis are also done by Oil Red O staining.

2.3.4. TUNEL assay

Tissue cell apoptosis was detected using a TUNEL fluorescence assay kit. Aorta and liver sections were treated with 0.3% Triton X-100, and after washing, the TUNEL detection solution was added for 1 h. Nuclei were counterstained with DAPI. Anti-fluorescence quenching sealing agents were added. The samples were visualized by confocal microscopy.

2.4. Western blot assay

Cellular proteins were extracted from HUVECs. Animal proteins were extracted from the whole aorta of $ApoE^{-/-}$ mice. BCA Protein Assay was used for quantification of total protein concentration and 50 μg of protein from each sample. Then the membranes were incubated at 4 °C with the primary mouse monoclonal antibody (Caspase-3, Bax, Bcl-2, or GAPDH) at a 1:1000 dilution overnight. After incubation, membranes were nurtured with secondary fluorescent antibody. Antigen-antibody immunocomplexes were visualized using the Odyssey imaging system.

2.5. Statistical analyses

All experiments were conducted in triplicates. Results are expressed as mean ± SEM in graphical representation. One-way ANOVA analysis was employed to analyze differences among groups. Kruskal-Wallis test was used to compare the differences between groups when the variance was not uniform. All p-values were considered significant when $p < 0.05$. Statistical analyses were performed using SPSS 19.0 software (SPSS, Inc., Chicago, IL, USA).

3. Results

3.1. ASD protected against H_2O_2-induced cytotoxicity in HUVEC

Initially, the cytotoxicity of ASD on HUVECs was measured using the CCK-8 assay. As presented in Fig. 1A, incubation of HUVECs with 50, 100, or 200 μM ASD for 24 h did not significantly affect cell viability ($p > 0.05$). However, treatment of HUVECs with 200–400 μM H_2O_2 for 24 h led to a concentration-dependent decrease in cell viability, when compared with the vehicle control group ($p < 0.05$; Fig. 1B; Cell viability: 68.77 ± 9.18%, 48.29 ± 6.44%, 27.06 ± 14.64% *vs.* vehicle control). Pretreatment of HUVECs with 50, 100, or 200 μM ASD significantly increased cell viability in a dose-dependent manner (Cell viability: 85.57 ± 0.9%, 94.16 ± 1.1%, 96.67 ± 1.8%) compared with H_2O_2 300 μM model group (48.29 ± 6.44%) (Fig. 1C). In order to confirm that the protective effect of ASD on endothelial cells was not due to reaction between ASD and H_2O_2 in the medium, we added ASD and H_2O_2 simultaneously in the medium, and the cell viability of the pretreated group was not significantly improved compared with the model group (Fig. 1D). These results indicated that ASD might protect HUVECs from oxidative stress-induced injury. Based on these results, for further experiments, H_2O_2 concentration of 300 μM, and ASD concentrations of 50, 100, and 200 μM were employed.

3.2. ASD inhibited H_2O_2-induced apoptosis in HUVECs

To assess whether the protective effects of ASD were associated with apoptosis in *in vitro*, HUVECs were exposed to different ASD concentrations (50, 100, or 200 μM) for 12 h before H_2O_2 treatment. ASD attenuated H_2O_2-induced apoptosis in a dose-dependent manner when the cells were treated with 300 μM H_2O_2. Correspondingly, DAPI staining results showed that apoptotic cells exhibited significantly enhanced condensation of nuclei in the H_2O_2 treatment group but it was decreased with ASD pretreatment (Fig. 1E). Flow cytometry with Annexin V-FITC/PI staining is used to analyze the degree of apoptosis quantitatively (Fig. 1F). Consistent with the DAPI staining assays, Annexin V-FITC/PI staining showed that pretreatment with ASD significantly decreased the number of apoptotic cells in response to H_2O_2 treatment (percent of apoptosis cells: 15.27 ± 0.3%, 8.93 ± 0.45%, 6.93 ± 1.8% *vs.* 26.07 ± 3.65% model group).

3.3. ASD inhibited H_2O_2-induced ROS in HUVECs

To explore the signaling pathways involved in H_2O_2-induced cellular apoptosis, HUVECs were treated with H_2O_2, and levels of cytoplasmic ROS were measured. The results showed that, compared with the vehicle control group, H_2O_2 (300 μM)-treated cells exhibited significantly increased fluorescence intensity (ROS levels) ($p < 0.05$). After pretreatment with ASD (50, 100, or 200 μM), H_2O_2-induced ROS generation was suppressed in a dose-dependent manner ($p < 0.05$, Fig. 2A and B. Percent of ROS positive cells in the group pretreated with ASD: 7.69 ± 0.66%, 4.15 ± 0.87%, 4.45 ± 0.21% *vs.* model group 11.84 ± 0.93%). We concluded that accumulation ROS likely led to HUVECs apoptosis. The anti-apoptotic mechanism of ASD is likely to be mediated by decreasing ROS levels.

3.4. ASD ameliorates the loss of mitochondrial membrane potential induced by H_2O_2 in HUVECs

We estimated ($\triangle\Psi m$) using the JC-1 probe to test whether suppression of mitochondrial function disruption was involved in the anti-apoptotic effects of ASD. Previous reports have shown that H_2O_2 induced the opening of the permeability transition pore (PTP) and significantly decreased the MMP [18]. HUVECs were incubated with H_2O_2 for 24 h, and consequently, the MMP was depolarized in H_2O_2-treated cells as shown by the increase of green fluorescence and the decrease of red fluorescence. Compared with the model group, pretreatment with different concentrations of ASD prevented the loss in $\triangle\Psi m$ as indicated by the suppression of green fluorescence and restoration of red fluorescence (Fig. 2C and D. Ratio of Red/Green Flourescence: 1.19 ± 0.17%, 3.04 ± 0.53%, 6.53 ± 0.86% *vs.* model group 0.65 ± 0.35%). Furthermore, pretreatment with ASD completely prevented the suppression of MMP and blocked the apoptotic effect of H_2O_2 completely.

3.5. ASD reduced the atherosclerotic plaque formation in the aorta of $ApoE^{-/-}$ mice

To assess the cytoprotective function of ASD in *in vivo*, we established an experimental $ApoE^{-/-}$ AS mice model. After 14 weeks of treatment, serum indexes (LDL-C, TC, TG, AST, and ALT) were measured. As shown in Supplementary Table 1, the serum levels of abovementioned indexes in $ApoE^{-/-}$ model group were remarkably higher than those in C57BL/6 control group. ASD (150 and 450 mg/kg/d), atorvastatin, and combined treatment significantly decreased the levels of these serum indexes when compared with $ApoE^{-/-}$ model group. We also evaluated the AS plaque formation in the experimental $ApoE^{-/-}$ mice. As shown in Fig. 3B, treatment with 50, 150, and 450 mg/kg/d ASD reduced the aortic plaque area to 18.98 ± 1.78%, 15.95 ± 1.59%, and 13.62 ± 1.55%, respectively. Atorvastatin treatment (plaque area: 13.62 ± 1.43%) and combined treatment (plaque area: 7.82 ± 1.29%) significantly lowered the serum levels compared with $ApoE^{-/-}$model group (35.41 ± 3.11%). Fig. 3C shows the aortic valve plaque area, compared with $ApoE^{-/-}$ model group (plaque area: 49.14 ± 1.46%), ASD group (50, 150, 450 mg/kg/d) (40.07 ± 1.54%, 33.38 ± 1.66%, 27.26 ± 3.59%), atorvastatin group (32.93 ± 2.94%), and combined group (30.82 ± 2.2%) exhibited significantly reduced plaque area. Oil Red O (Fig. 3D) staining revealed that the plaque areas of the ASD (50, 150, 450 mg/kg/d) group are 12.66 ± 0.71%, 10.09 ± 1.68%, 7.44 ± 0.95%, respectively, and those of atorvastatin and combined group are 10.91 ± 0.79% and 5.79 ± 0.76%, respectively. The plaque areas were significantly lower than $ApoE^{-/-}$ model group (22.08 ± 1.49%). These results showed that ASD (150, 450 mg/kg/d) and combined treatment might elicit better effect on inhibition of atherosclerotic plaque formation.

3.6. Effects of ASD on oxidative stress and lipid deposition in the liver of $ApoE^{-/-}$ mice

Our study indicated that there was a significant reduction in GSH production, and SOD and CAT activities in liver and vascular tissues of $ApoE^{-/-}$ model mice. After 14 weeks of treatment, ASD (450 mg/kg/d) significantly increased the levels of GSH, CAT, and SOD. Combined treatment and ASD treatment (150 mg/kg/d) increased the levels of GSH and CAT (Supplementary Table 2**)**. Fig. 4A–B shows that the lipid deposition in the liver was significantly increased in $ApoE^{-/-}$ model mice (16.85 ± 1.12%). However, lipid deposition was significantly reduced after treatment with ASD (11.16 ± 0.67%, 8.15 ± 1.48%, 7.47 ± 1.14%), atorvastatin treatment (9.44 ± 1.09%) or combined treatment (7.78 ± 0.57%). To ascertain relationship between vascular lipid deposition and oxidative stress, we evaluated the aortic oxidative stress markers, SOD, CAT, and GSH (Supplementary Table 3). We found that ASD increased the intravascular production of antioxidant enzymes while inhibiting lipid deposition, and thus, increased the ability of blood vessels to resist oxidative stress. Finally, we concluded that treatment with ASD (150 and 450 mg/kg/d) enhanced the antioxidant defenses in the liver and the metabolism of lipids in the liver.

3.7. Administration of ASD reduced aortic and liver apoptosis

ASD has been proven to reduce HUVECs apoptosis in *in vitro*. We

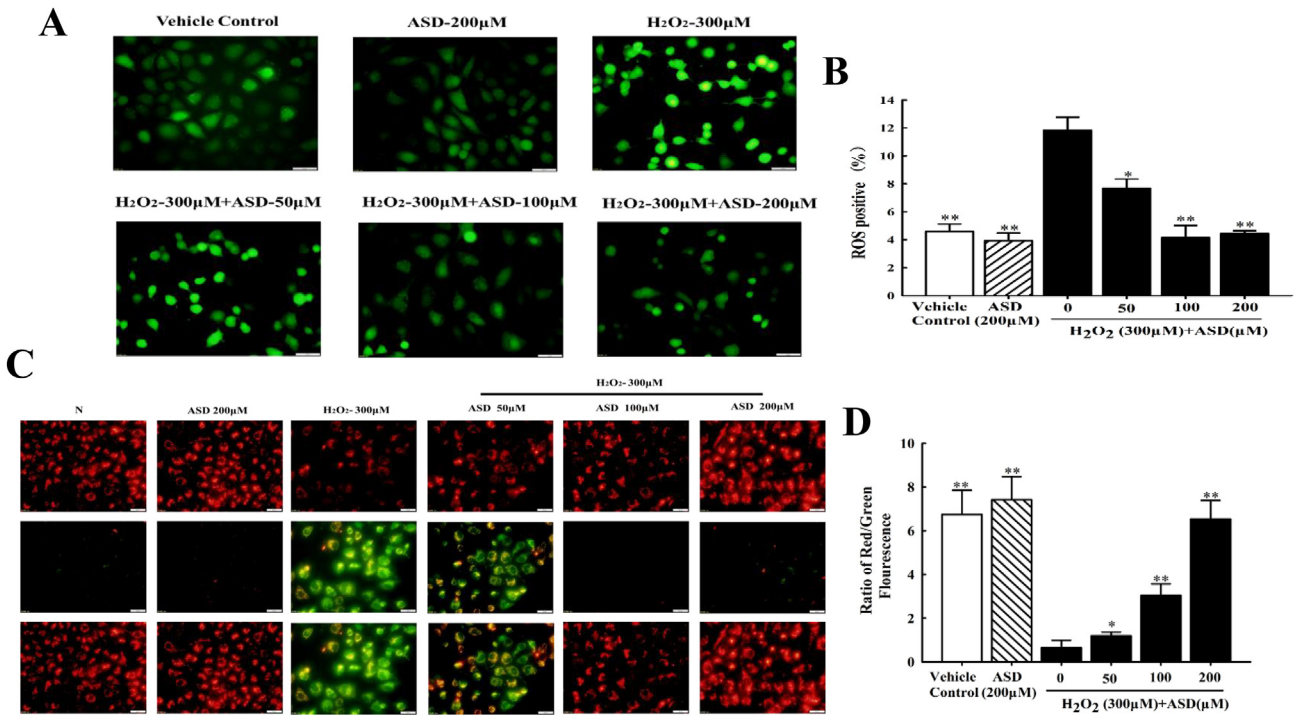

Fig. 2. Effects of ASD on H_2O_2-induced ROS production and mitochondrial membrane potential in HUVECs.
Cells were pre-treated with different concentrations of ASD for 12 h, followed by treatment with 300 μm H_2O_2 for 24 h. (A) ROS levels in HUVECs exposed to H_2O_2 and ASD were detected using DCFH-DA staining; magnification: 400×. (B) Analysis of the fluorescence intensity of cells. (C) Determination of △Ψm was conducted using JC-1 probe and fluorescence was determined with fluorescence microscope. Red fluorescence was emitted by JC-1 aggregates in healthy mitochondria with polarized inner mitochondrial membranes, while green fluorescence was emitted by cytosolic JC-1 monomers and indicated △Ψm dissipation. Merged images indicated the co-localization of JC-1 aggregates and monomers. Magnification: 400×. (D) △Ψm in each group was calculated as the ratio of red to green fluorescence. All results are presented as mean ± SEM, and images were representative of at least three independent experiments. $^*p < 0.05$, $^{**}p < 0.01$ *versus* H_2O_2-treated group. (n = 3). (For interpretation of the references to colour in this figure legend, the reader is referred to the Web version of this article.)

performed TUNEL analysis to evaluate the apoptosis in *in vivo*. We found that the cellular apoptosis in the aortic root, which was subjected to with ASD treatment, atorvastatin treatment, and combined treatment is reduced (Fig. 5A–B). The proportions of apoptotic cells in ASD groups were 5.70 ± 1.01%, 3.81 ± 0.41%, 2.11 ± 0.45% respectively for different doses, and in atorvastatin treatment and combines treatment groups were 2.21 ± 0.19% and 2.11 ± 0.23%, respectively; however, the proportion of apoptotic cells in $ApoE^{-/-}$ model group reached to 7.76 ± 1.71%. Furthermore, in the liver, we found that the apoptosis of hepatocytes was significantly reduced after same treatment, The proportion of apoptotic cells in $ApoE^{-/-}$ model group was 22.43 ± 2.57%, in ASD groups were 19.15 ± 0.58%, 13.59 ± 2.32%, and 6.82 ± 0.71%, respectively for different doses, in atorvastatin and combine treatment groups were 7.79 ± 0.72% and 5.72 ± 0.73% (Fig. 5C–D).

3.8. ASD inhibited H_2O_2-induced HUVEC apoptosis by increasing levels of Bcl-2 family proteins and decreasing Caspase-3 activation

To evaluate whether ASD inhibited the apoptosis responses through Bax-Bcl-2-Caspase-3 axis in HUVECs, we focused our attention on assessing the levels of several Bcl-2 pathway-related proteins. As shown in Supplementary Fig. 2, pre-incubation with ASD inhibited H_2O_2-induced increase in cytoplasmic levels of Bax/Caspase-3 and promoted Bcl-2 expression in a dose-dependent manner.

4. Discussion

Atherosclerosis is a complex, chronic process that is initiated at sites of endothelial cell injury. Injured endothelial cells can cause exposure of the subendothelial matrix and facilitate plaque formation [3]. When the blood lipid level in the body is increased, endothelial cells are widely exposed to a high-fat environment, and thus, they continuously undergo lipid degradation, and a large amount of H_2O_2 in produced during lipid aerobic metabolism. H_2O_2 is an independent risk factor for cardiovascular diseases, even moderate H_2O_2 levels being independently responsible for the development of premature atherosclerosis [7]. H_2O_2 is a highly reactive lipid metabolite known to induce cellular injury, cytotoxicity, and apoptosis in endothelial cells [19]. In the present study, we demonstrated that ASD prevented atherosclerosis progression and inhibited H_2O_2-induced apoptosis in HUVECs by decreasing the intracellular ROS overproduction, inhibiting the loss of mitochondrial membrane potential, and preserving Bcl-2, Bax/Caspase-3 signaling pathway.

In a recent study, H_2O_2 has been shown to induce apoptosis in HUVECs [20]. Annexin V-FITC/PI staining showed that treatment with a concentration of 300 μM H_2O_2 for 24 h significantly increased the degree of apoptosis in HUVECs and pretreatment with ASD reduced the production of ROS and suppressed cellular injury in a dose-dependent manner. The drug concentrations of ASD and time point for dose administration was based on a previous study result, which showed that pretreatment with 50–200 μM ASD significantly alleviate H_2O_2-induced retinal endothelial cell damage.

In the atheromatous process, overproduction of ROS has been regarded as the major cellular response to AS [9]. ROS are the main products of oxidative stress, which can activate lipid peroxidation and aggravate mitochondrial dysfunction, cellular apoptosis, and ultimately lead to death. Mitochondria play a key role in triggering apoptotic events by regulating the production of cellular energy, and is a target of ROS and a source for the additional ROS generation [21]. More importantly, a previous report showed that H_2O_2-induced apoptosis in HUVECs primarily through the overproduction of reactive oxygen

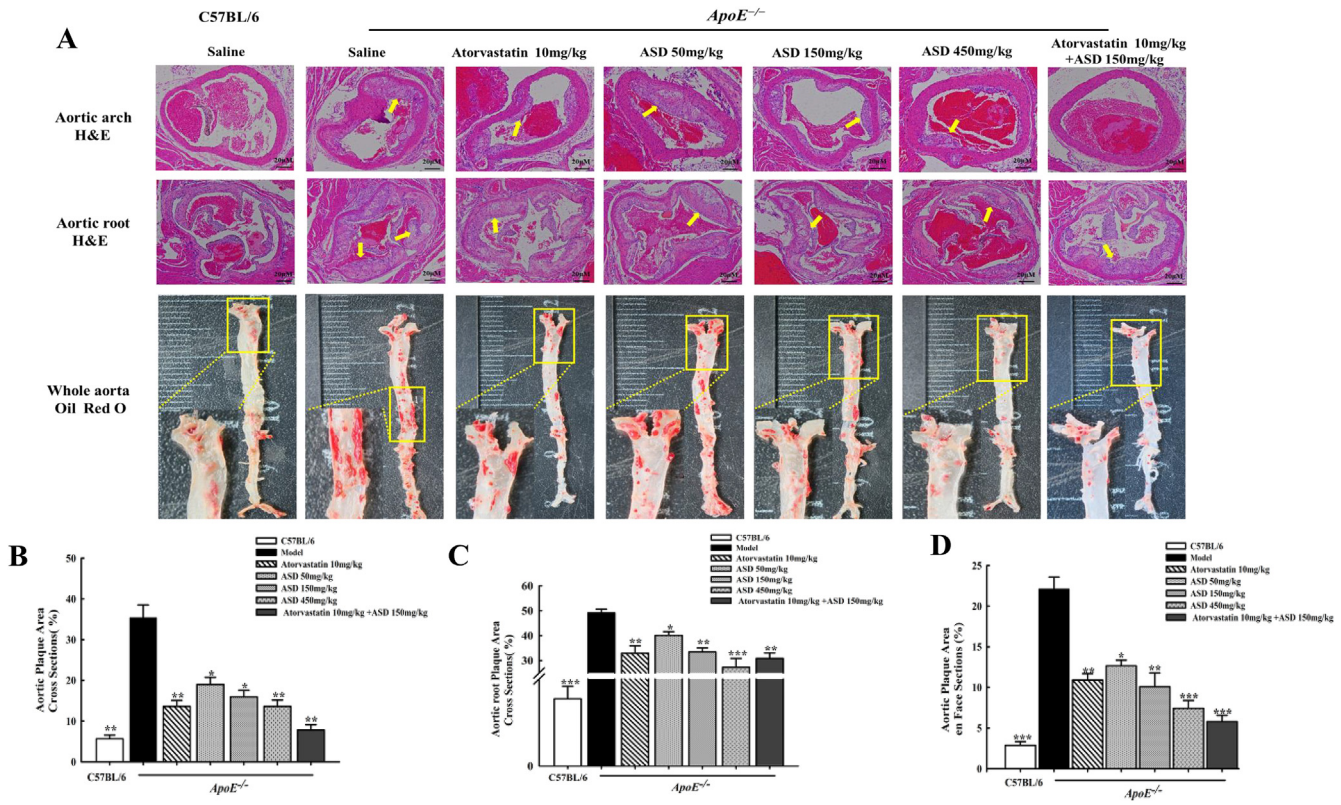

Fig. 3. ASD inhibits the formation of atherosclerotic lesions and increases the activity of antioxidant enzymes in aorta.
At least five sections for each animal for one treatment group were evaluated, and the lesions were evaluated from six different mice. (A) Representative photographs of aortic lesions (top), and HE-stained aortic root lesions (middle). Magnification: 200×. Oil Red O staining of the whole aortic area (bottom). (B) Areas of the aortic lesion were expressed as percentage of aorta areas. (C) Areas of aortic root lesion were expressed as percentage of total areas. (D) Oil red area occupies the percentage of aortic area. Bars represent mean ± SEM (n = 6 animals/group). $*p < 0.05$ $**p < 0.01$ and $***p < 0.001$ compared to the $ApoE^{-/-}$(HFD) model group. (For interpretation of the references to colour in this figure legend, the reader is referred to the Web version of this article.)

species (ROS) [18]. Therefore, we were interested in exploring whether ASD could affect H_2O_2-induced ROS generation. Our results showed that pretreatment with ASD significantly inhibited ROS generation induced by H_2O_2 in HUVECs and maintained mitochondrial membrane potential at a steady state. The above results indicated that the anti-apoptotic features of ASD were attributed to its antioxidant capacity in H_2O_2-induced damage of HUVECs. In addition, the Bcl-2 family is composed of central regulators of cell survival or death after apoptotic stimulation. Bax is a pro-apoptotic protein of the Bcl-2 family that targets the mitochondria causing the release of cytochrome *c* from mitochondria [22]. Bcl-2, an anti-apoptotic member of the Bcl-2 family, maintains the mitochondria membrane potential preventing the release of such apoptotic signaling molecules. Our results were in agreement with previous studies showing ROS as an important upstream signal molecule in H_2O_2-induced apoptosis. Pre-incubation with ASD downgraded the H_2O_2-induced levels of caspase-3 and upregulated the Bcl-2/Bax ratio, confirming that ASD might protect against H_2O_2-induced cell apoptosis by regulating the production of ROS in mitochondria.

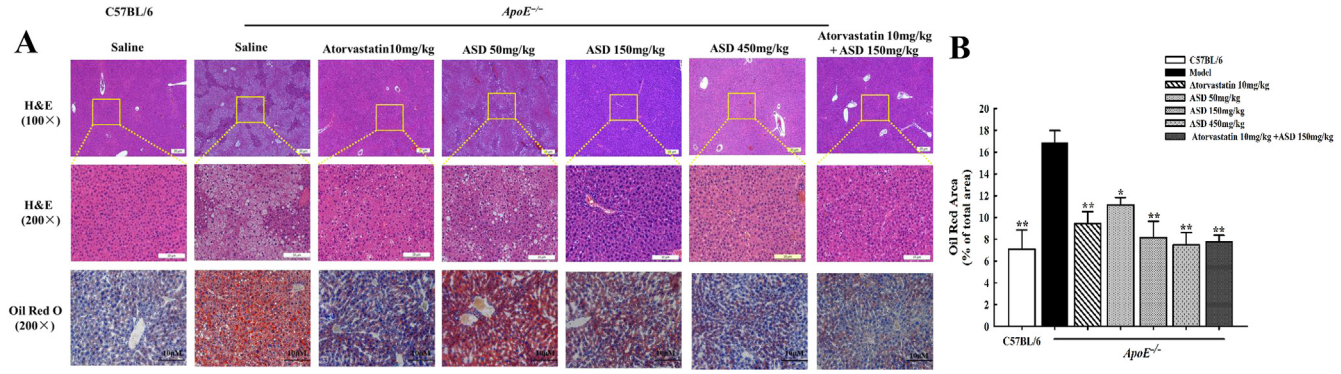

Fig. 4. Representative histological images of livers from experimental groups after 14 weeks of HFD and effects of ASD treatment on activities of antioxidant enzymes in the liver tissue of $ApoE^{-/-}$(HFD) mice.
(A) Representative HE staining of liver tissue sections. Magnification: 100×. (top). Representative HE staining of liver tissue sections. Magnification: 200×. (middle). Oil Red-O staining of lipid accumulation in liver. Magnification: 200×. (bottom). (B) Oil red area as a percentage of total area, (n = 6); $*p < 0.05$, $**p < 0.01$ $***p < 0.001$ compared with the $ApoE^{-/-}$(HFD) group. (For interpretation of the references to colour in this figure legend, the reader is referred to the Web version of this article.)

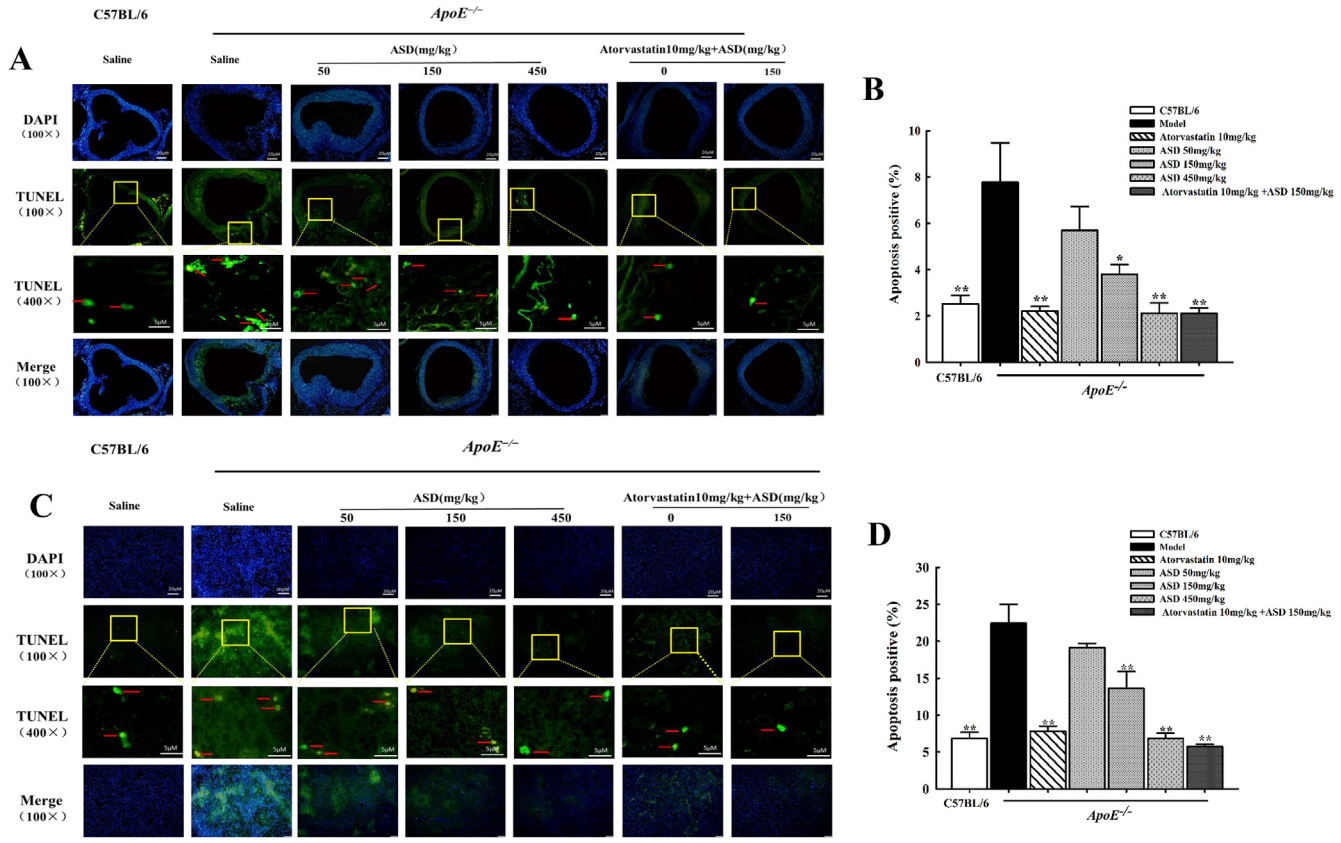

Fig. 5. Liver and aortic roots were stained with TUNEL reaction to reveal cells undergoing DNA fragmentation.
(A) Sections of aortic root, and (C) liver tissues were processed for TUNEL assay to detect apoptosis of aortic root and liver. Nuclei were stained with DAPI (blue), and the section undergoing TUNEL assay was stained in green. Magnification: 100×. Data are expressed as mean ± SEM (n = 6). $*p < 0.05$, $**p < 0.01$ *vs.* the $ApoE^{-/-}$(HFD) group. (For interpretation of the references to colour in this figure legend, the reader is referred to the Web version of this article.)

Akebia Saponin D is a natural compound isolated from the well-known traditional Chinese herb Dipsacus asper wall. Many previous studies have explored the mechanisms of ASD in different diseases. Gong et al. have demonstrated that ASD could decrease the development and progression of NAFLD by alleviating hepatic steatosis targeted at the modulation of autophagy and exerts hepatoprotective effects through mitochondria. Zhou et al. proposed that ASD inhibited excessive Ca^{2+} influx, reducing additional LDH leakage, and protecting PC-12 cells against amyloid-beta-induced cytotoxicity. J et al. believed that ASD induces apoptosis by inducing NO production in U937 cells. Li et al. reported that ASD inhibits hypoxia-induced apoptosis by activating PI3K-AKT and CREB pathway in cardiomyocytes [23]. Most of cytotoxicity caused by ASD treatment occurred in tumor cells. Conversely, the protective role of ASD in normal cells (cardiomyocytes, hepatocytes, and human umbilical vein endothelial cells) was reported as well. ASD is a multi-target drug and the different pharmacological effects of ASD are likely to be caused by different target proteins in different cells.

Here, the effects of ASD on serum lipids were first studied on $ApoE^{-/-}$ mice. We found that ASD could significantly lower serum levels of ALT, AST, TG, TC, and LDL-C compared to those of the $ApoE^{-/-}$ model group and lipid accumulation in the liver was also significantly reduced. Meanwhile, ASD exhibited protective effects against oxidative damage by increasing the levels of anti-oxidant enzymes, such as SOD, GSH, and CAT in the liver of $ApoE^{-/-}$ mice. Furthermore, ASD treatment substantially decreased lipid deposition and the area of atherosclerosis lesion in artery root, which corresponds to its anti-atherosclerosis effect. Thus, in the future, ASD can be used as a drug used for preventing the formation of atherosclerosis. According to these experiments, 150 and 450 mg/kg/d of ASD exhibit therapeutic action. Assuming that the weight of an adult human is 60 kg, he/she has to take 0.9 g/d or 2.7 g/d of ASD. Although 450 mg/kg ASD is effective in inhibiting the formation of atherosclerosis, it is considered that during translation to the clinic may reduce the dose according to the patient's compliance due to the high dose (2.7 g/d). In the lipid-lowering proposal provided by the latest guidelines [24,25], statins remain the first choice for treatment, but the liver toxicity of statins cannot be ignored. The combination of atorvastatin (10 mg/kg/d) and ASD (150 mg/kg/d) can effectively reduce blood lipid (TG, TC, and LDL-C), decrease ALT and AST activities, and increase anti-oxidative markers (GSH, CAT, and SOD) in liver and vascular tissue. Simultaneously, the effect on inhibition of lipid deposition in vascular and hepatic tissue was better than statin alone. Therefore, in our opinion, the combinational therapeutics may reach greater clinical benefit in less time.

4.1. Conclusion

Conclusively, *in vitro* study showed that ASD prevented H_2O_2-induced apoptosis in HUVECs by reducing ROS overproduction, inhibiting oxidative stress, suppressing apoptotic signaling cascades (Bax and Caspase-3), promoting the expression of anti-apoptotic proteins (Bcl-2). *In vivo* studies provided new insight into the mechanisms of ASD in atherosclerosis, which was predominantly mediated through attenuating endothelial dysfunction and enhancing anti-oxidative enzyme, and reduction of lipid deposition in liver and vascular tissue. These findings provided further evidence that ASD might be a potential agent involved in the clinical application of cardiovascular complications.

Conflicts of interest

The authors declared they do not have anything to disclose regarding conflict of interest with respect to this manuscript.

Author contributions

The study was designed by Lili Gong and Lihong Liu; the experiments were conducted by Song Yang. All authors contributed to the writing of the paper.

Financial support

This study was supported by Beijing Municipal Natural Science Foundation (No. 7172085), Beijing Municipal Administration of Hospitals' Youth Programme (No. QML20150302), the National Natural Science Foundation of China (No.81302822).

Appendix A. Supplementary data

Supplementary data to this article can be found online at https://doi.org/10.1016/j.atherosclerosis.2019.04.202.

References

[1] E.J. Benjamin, S.S. Virani, C.W. Callaway, et al., Heart disease and stroke statistics-2018 update: a report from the American heart association, Circulation 137 (2018) e67–e492.
[2] T.A. Gaziano, A. Bitton, S. Anand, et al., Growing epidemic of coronary heart disease in low- and middle-income countries, Curr. Probl. Cardiol. 35 (2010) 72–115.
[3] P.N. Hopkins, Molecular biology of atherosclerosis, Physiol. Rev. 93 (2013) 1317–1542.
[4] G.K. Hansson, Hermansson, A the immune system in atherosclerosis, Nat. Immunol. 12 (2011) 204–212.
[5] N.V.K. Pothineni, S. Subramany, K. Kuriakose, et al., Infections, atherosclerosis, and coronary heart disease, Eur. Heart J. 38 (2017) 3195–3201.
[6] M. Mudau, A. Genis, A. Lochner, et al., Endothelial dysfunction: the early predictor of atherosclerosis, Cardiovasc. J. Afr. 23 (2012) 222–231.
[7] T. Hsiai, J.A. Berliner, Oxidative stress as a regulator of murine atherosclerosis, Curr. Drug Targets 8 (2007) 1222–1229.
[8] M.A. Incalza, R. D'Oria, A. Natalicchio, et al., Oxidative stress and reactive oxygen species in endothelial dysfunction associated with cardiovascular and metabolic diseases, Vasc. Pharmacol. 100 (2018) 1–19.
[9] E. Di Marco, S.P. Gray, P. Chew, et al., Pharmacological inhibition of NOX reduces atherosclerotic lesions, vascular ROS and immune-inflammatory responses in diabetic *Apoe*(-/-) mice, Diabetologia 57 (2014) 633–642.
[10] S. Maharjan, M. Oku, M. Tsuda, et al., Mitochondrial impairment triggers cytosolic oxidative stress and cell death following proteasome inhibition, Sci. Rep. 4 (2014) 5896.
[11] E.P. Yu, M.R. Bennett, The role of mitochondrial DNA damage in the development of atherosclerosis, Free Radic. Biol. Med. 100 (2016) 223–230.
[12] S. Li, Y. Hong, X. Jin, et al., Agkistrodon acutus-purified protein C activator protects human umbilical vein endothelial cells against H2O2-induced apoptosis, Pharmaceut. Biol. 54 (2016) 3285–3291.
[13] X.M. van Delden, R. Huijgen, K.H. Wolmarans, et al., LDL-cholesterol target achievement in patients with heterozygous familial hypercholesterolemia at Groote Schuur Hospital: minority at target despite large reductions in LDL-C, Atherosclerosis 277 (2018) 327–333.
[14] Y. Wang, J. Shen, X. Yang, et al., Akebia saponin D reverses corticosterone hypersecretion in an Alzheimer's disease rat model, Biomed. Pharmacother. 107 (2018) 219–225.
[15] Y. Niu, Y. Li, H. Huang, et al., Asperosaponin VI, a saponin component from Dipsacus asper wall, induces osteoblast differentiation through bone morphogenetic protein-2/p38 and extracellular signal-regulated kinase 1/2 pathway, Phytother Res. : PTR 25 (2011) 1700–1706.
[16] C. Li, Z. Liu, J. Tian, et al., Protective roles of Asperosaponin VI, a triterpene saponin isolated from Dipsacus asper Wall on acute myocardial infarction in rats, Eur. J. Pharmacol. 627 (2010) 235–241.
[17] L.L. Gong, G.R. Li, W. Zhang, et al., Akebia saponin D decreases hepatic steatosis through autophagy modulation, J. Pharmacol. Exp. Ther. 359 (2016) 392–400.
[18] R. Han, F. Tang, M. Lu, et al., Astragalus polysaccharide ameliorates H2O2-induced human umbilical vein endothelial cell injury, Mol. Med. Rep. 15 (2017) 4027–4034.
[19] S.J. Wilson, Keenan, AK Role of hemin in the modulation of H2O2-mediated endothelial cell injury, Vasc. Pharmacol. 40 (2003) 109–118.
[20] Y. Oh, C.B. Ahn, N.Y. Yoon, et al., Protective effect of enzymatic hydrolysates from seahorse (Hippocampus abdominalis) against H2O2-mediated human umbilical vein endothelial cell injury, Biomed. Pharmacother. 108 (2018) 103–110.
[21] Z. Huang, L. Liu, J. Chen, et al., JS-K as a nitric oxide donor induces apoptosis via the ROS/Ca(2+)/caspase-mediated mitochondrial pathway in HepG2 cells, Biomed. Pharmacother. 107 (2018) 1385–1392.
[22] R.W. Birkinshaw, P.E. Czabotar, The BCL-2 family of proteins and mitochondrial outer membrane permeabilisation, Semin. Cell Dev. Biol. 72 (2017) 152–162.
[23] C. Li, J. Tian, G. Li, et al., Asperosaponin VI protects cardiac myocytes from hypoxia-induced apoptosis via activation of the PI3K/Akt and CREB pathways, Eur. J. Pharmacol. 649 (2010) 100–107.
[24] M.D. Miedema, Z.A. Dardari, S. Kianoush, et al., Statin eligibility, coronary artery calcium, and subsequent cardiovascular events according to the 2016 United States preventive services task force (USPSTF) statin guidelines: MESA (Multi-Ethnic study of atherosclerosis), J. Am. Heart Assoc. 7 (2018) e008920.
[25] M. Arca, D. Ansell, M. Averna, et al., Statin utilization and lipid goal attainment in high or very-high cardiovascular risk patients: insights from Italian general practice, Atherosclerosis 271 (2018) 120–127.